JOURNAL OF COMPUTATIONAL PHYSICS 102, 236–251 (1992)

Absorbing Boundary Conditions, Difference Operators, and Stability

R. A. RENAUT*

Arizona State University, Tempe, Arizona 85287-1804

Received October 11, 1989; revised August 8, 1991

In this paper we present a review of some of the methods currently used for solving the absorbing boundary problem for the two-dimensional scalar wave equation. We show the relationship between the methods of Lindman and Clayton and Engquist. Through this relationship we can derive discretizations of any rational approximation to the one-way wave equation. We prove that, for all the cases considered here, which can be solved in a manner similar to Lindman's approach, the bounds imposed on the Courant number for stability at the boundary are no more severe than the bound $1/\sqrt{2}$ required for stability of the interior scheme. These bounds are, however, necessary but not sufficient. We also compare the methods reviewed numerically. It is demonstrated that Lindman's scheme is no better than a sixth-order approximation of Halpern and Trefethen. For low-order approximations, Higdon's one-dimensional equations are satisfactory, but as the order increases the two-dimensional form of the equations, as derived by Halpern and Trefethen, is preferable.

INTRODUCTION

The numerical solution of the wave equation on an infinite domain requires that the domain be cut to obtain the computational domain. In this process artificial boundaries are introduced. Ideally, these boundaries absorb all incident energy. The absorbing boundary problem thus involves imposing boundary conditions in a way that best realises this objective. There are many techniques for reducing the amount of the reflected energy. Cerjan *et al.* (1985) [1] considered enlarging the computational domain and applying a damping mechanism in the artificial part of the domain. Although effective, this method is costly, particularly for extension to higher dimensions. Other techniques for reducing spurious reflection have been proposed by many authors including Higdon [8, 10], Smith [19], Goldstein [4], and Keller and Givoli [12]. Alternative approaches based on approximations to the one-way wave equation have been investigated by many authors, including Lindman [15], Clayton and Engquist [2], and Halpern and Trefethen [6]. These authors have solved an equation at the boundary derived from approximations to the one-way wave equation for which energy flows in one direction only. Here we will compare some of the results obtained using different equations at the boundary. Our purpose is to demonstrate that the choice of discretization of the equation is crucial for a stable scheme.

In an earlier paper, Renaut and Petersen [16], compared the wide-angle absorbing boundary conditions of order two derived by Halpern and Trefethen [6]. These boundary conditions also include the familiar paraxial approximation of order two found by Clayton and Engquist [2]. The discretization of these conditions that was adopted was the same form as that proposed by Clayton and Engquist [2]. Renaut and Petersen observed that although this discretization imposes no restriction on the Courant number, ratio time step to space step, for the paraxial equation this may not be the case for all other second-order conditions. There is a bound on the allowable Courant number, μ, which is determined by the coefficients of the underlying rational approximation. In some cases this bound is more severe than the $1/\sqrt{2}$ bound imposed by the stability of the interior scheme. Here, we propose a discretization for which no restriction on μ occurs due to the boundary scheme. Furthermore, we look at higher order approximations and find stable discretizations for the boundary equations.

The schemes proposed here are compared with the boundary operators suggested by Higdon [8, 10]. In each case, equivalence between a Halpern and Trefethen [6] equation and a Higdon [8, 10] operator exists in terms of the theoretical reflection coefficient. The implementation is, however, quite different. Higdon's operators are completely one-dimensional and are first-order approximations in space and time. The equations of Halpern and Trefethen are two-dimensional and are solved with second-order difference operators. Higdon [8, 10] performed a stability analysis of his operators and found an inequality which the coefficients must obey for stability. Here we find necessary bounds on the Courant number, in terms of the coefficients of the operators, above which stability is not possible.

Lindman's [14] approach is similar to that of Clayton

* The work of the author was supported by National Science Foundation Grant ASC 8812147 and an American Chemical Society Petroleum Fund Grant 20681-G2.

0021-9991/92 $5.00

and Engquist [2] in that it involves an approximation to a function at the boundary. We review the derivation of Lindman's scheme and show that it is actually very similar to Halpern and Trefethen's ideas [6]. Randall [15] demonstrated that Lindman's scheme is more effective than the paraxial approximation for the solution of the elastic wave equation. This is not surprising because Lindman's scheme amounts to a twelfth-order approximation as compared to the paraxial approximation which is second order.

Higdon [8] conjectured that the third paraxial approximation requires an implicit discretization. We show that this is not the case. In fact, any of the Halpern and Trefethen [6] approximations can be reformulated in a Lindman-type setting for which an explicit difference operator is immediately available. It turns out that these operators are exactly those which we have investigated for the discretization of the higher-order approximations, for which the necessary condition for stability is no more severe than the stability condition of the interior scheme.

Higdon [10] observed that his schemes may exhibit instability when the operator is composed of three or more factors. This mild unstable behavior was stimulated by an accidental incompatibility in some of the numerical computations. In [8] it was shown that the incompatibility was more troublesome for low frequency data and arises due to the existence of generalized eigensolutions with frequency and wavenumber zero. We show in Section 5 that this generalized eigensolution also exists for the methods presented here. In fact, it is found with any boundary condition containing derivatives and no undifferentiated terms, since a constant automatically satisfies the boundary condition. Furthermore, also in Section 5, we show that the methods in this paper do allow for generalized eigensolutions at other frequencies and wavenumbers. These are, therefore, again subject to incompatibility. In general the potential for incompatibility is reduced if fewer points away from the boundary are used in the approximation of the boundary condition. The methods we present here have the advantage of reducing this number, marginally, as compared to the boundary operators in [8]. Given the disadvantage of the greater number of generalized eigensolutions of the methods here it is not clear whether the operators in [8] or these here are more vulnerable to incompatibility.

In Section 2 we review the derivation of the rational approximation to the one-way wave equation and present difference operators for approximations up to order six. In Section 3 we present the Higdon [8, 10] operators and in Section 4 we review Lindman's [14] approach. The stability of the operators in Section 2 is considered in Section 5 and in Section 6 we compare all methods numerically. Section 7 is a short concluding section, in which the conclusions from the preceding theoretical and numerical investigations are given.

The numerical computations demonstrate that the bounds on Courant number found in Section 5 are correct. Furthermore, difference schemes which are designed in a symmetric manner do not impose any restriction on the Courant number which is greater than that imposed by stability of the interior scheme. The existence of generalised eigensolutions is, however, not covered by our theory. Numerical searches show that in several cases these do exist but their effects are only seen in a scheme for which the operator is not symmetric in time. For minimal reflection the rational approximation approach in [2, 6, 14] does not appear to be significantly better than the operator approach of Higdon [8, 10], but the fact that rational approximation uses fewer points perpendicular to the boundary may be advantageous for high-order approximations. Also a sixth-order rational approximation [6] performs about the same as the twelfth-order Lindman scheme.

2. ONE-WAY WAVE EQUATIONS

Consider the second-order wave equation

$$u_{tt} = c^2(u_{xx} + u_{yy}) \tag{2.1}$$

for $x > 0$, $y \in \mathbf{R}$, $t > 0$, and $u = u(x, y, t)$. The solutions of (2.1) are plane waves which travel in every direction in two dimensions. Substitution of

$$u(x, y, t) = e^{i(\omega t + \xi x + \eta y)} \tag{2.2}$$

into (2.1), where ω is the frequency and ξ and η are wave numbers leads to the dispersion relation

$$\omega^2 = c^2(\xi^2 + \eta^2). \tag{2.3}$$

A wave with wave numbers ξ and η travels at the velocity $c(-\xi/\omega, -\eta/\omega) = c(-\cos\theta, -\sin\theta)$, where θ is the angle measured counterclockwise from the positive x-axis of the normal to the wave. Suppose that there is an artificial boundary at $x = 0$. Ideally, this boundary should only allow those waves which travel to the left, $|\theta| \leqslant 90°$, to be propagated. Such waves satisfy the dispersion relation

$$\xi = \frac{\omega}{c}\sqrt{1 - s^2}, \tag{2.4}$$

where $s = \eta c/\omega = \sin\theta \in [-1, 1]$, and $\theta \in [-90°, 90°]$. Equation (2.4) is the positive root of (2.3), and because of the square root it is not the dispersion relation of a partial differential equation.

In order to nearly satisfy (2.4) at the boundary practical one-way wave equations are obtained by finding a rational

approximation $r(s)=P_m(s)/Q_n(s)$ to the square root function. Here P_m and Q_n are polynomials of degree m and n in s, respectively. Then (2.4) is replaced by

$$\xi=\frac{\omega r(s)}{c} \tag{2.5}$$

or, equivalently,

$$\sum_{j=0}^{n} q_j\left(\frac{\eta c}{\omega}\right)^j \xi c=\omega \sum_{j=0}^{m} p_j\left(\frac{\eta c}{\omega}\right)^j. \tag{2.6}$$

To clear the ω in the denominator we multiply by the factor ω^K, $K=\max\{n, m-1\}$ and then we have the dispersion relation for the differential equation

$$\sum_{j=0}^{n} q_j c^{j+1} u_{y^j t^K - j x}=\sum_{j=0}^{m} p_j c^j u_{y^j t^{K-j+1}}. \tag{2.7}$$

To study the reflective properties of the differential equation at the boundary, consider a wave which consists of both a leftgoing and a rightgoing part,

$$u(x, y, t)=A_I e^{i(\xi x+\eta y+\omega t)}+A_R e^{i(-\xi x+\eta y+\omega t)},$$

where A_I and A_R are the amplitudes of the incident and reflected parts, respectively. This wave satisfies (2.7) at the boundary and therefore the ratio of A_R to A_I is given by

$$\frac{A_R}{A_I}=-\frac{[r(s)-\sqrt{1-s^2}]}{[r(s)+\sqrt{1-s^2}]} \tag{2.8}$$

which is the reflection coefficient for (2.7).

Now Trefethen and Halpern [23] proved that only the approximations with $m=n$ or $m=n+2$ lead to well-posed problems. Halpern and Trefethen [6] found approximations $r(s)$, where $r(s)$ is assumed to be even, $r(s)=r(-s)$, with $m=n$ and $m=n+2$ by a variety of techniques. The techniques that they used to find these approximations are fully defined in [6]. We have labelled the approximations according to the method of approximation that was used to find it, for example, the Padé approximations were found using Padé approximations for (2.5). In Table I we give the coefficients of these approximations for $k=1, ..., 4$, $k=\frac{1}{2}(m+n+2)$. Note that because the only choices for m and n are $m=n$ or $m=n+2$ and because m and n are both even, the value of k determines m and n uniquely. When $m=n$, k is odd, $k=n+1$, and when $m=n+2$, k is even, $k=n+2$. The coefficients that are not listed in Table I are, therefore, zero, except $q_0=1$ in every case. These correspond to approximations with order 0, 2, 4, and 6, respectively. Their reflection coefficients are drawn in Fig. 1.

TABLE I

Coefficients of One-Way Wave Equations

k	Padé	L_α^∞	Chebyshev points	L^2	C-P	Newman points	L^∞
1	1.00000	0.99240	0.70711	0.78540	0.63662	0.00000	0.50000
	0.00000	0.00000	0.00000	0.00000	0.00000	0.00000	0.00000
	0.00000	0.00000	0.00000	0.00000	0.00000	0.00000	0.00000
	0.00000	0.00000	0.00000	0.00000	0.00000	0.00000	0.00000
2	1.00000	1.00023	1.03597	1.03084	1.06103	1.00000	1.12500
	−0.50000	−0.51555	−0.76537	−0.73631	−0.84883	−1.00000	−1.00000
	0.00000	0.00000	0.00000	0.00000	0.00000	0.00000	0.00000
	0.00000	0.00000	0.00000	0.00000	0.00000	0.00000	0.00000
3	1.00000	0.99973	0.99650	0.99250	0.99030	1.00000	0.95651
	−0.75000	−0.80864	−0.91296	−0.92233	−0.94314	−1.00000	−0.94354
	0.00000	0.00000	0.00000	0.00000	0.00000	0.00000	0.00000
	−0.25000	−0.31657	−0.47258	−0.51084	−0.55556	−0.66976	−0.70385
4	1.00000	1.00015	1.00034	1.00227	1.00161	1.0000	1.01773
	−1.00000	−1.16394	−1.27073	−1.37099	−1.37170	−1.48698	−1.59644
	0.12500	0.22308	0.29660	0.38178	0.38027	0.48698	0.57976
	−0.50000	−0.65974	−0.76017	−0.83407	−0.84000	−0.91384	−0.94301

Note. Coefficients are listed in the pattern p_0, p_2, p_4, q_2.

Renaut and Petersen [16] compared the $k=2$ equations which have differential equation

$$u_{xt}=\frac{p_0}{c}u_{tt}+cp_2u_{yy}. \tag{2.9}$$

For $p_0=1$ and $p_2=-\frac{1}{2}$ this is the second-order paraxial approximation for which Clayton and Engquist [2] proposed the discretization

$$D_+^x D_0^t u_{nk}^0-\frac{p_0}{2c}D_+^t D_-^t(u_{nk}^0+u_{nk}^1)$$

$$-\frac{p_2 c}{2}D_+^y D_-^y(u_{n+1k}^1+u_{n-1k}^0)=0. \tag{2.10}$$

Here D_+^q, D_-^q, and D_0^q are standard forward, backward, and central difference operators, u_{nk}^j is an approximation to $u(j\Delta x, k\Delta y, n\Delta t)$, Δx, Δy are gridsizes in x and y directions and Δt is the timestep. This operator has a truncation error $O(\Delta x^2)+O(\Delta t^2)+O(\Delta x\,\Delta t)$ because the first-order terms cancel. Renaut and Petersen [16] proved that $\mu<-1/2p_2$ is necessary for stability, where $\mu=c\,\Delta t/\Delta x$ is the Courant number. For all but the Padé and L_α^∞ approximations this bound on μ is more restrictive than the von Neumann stability bound $\mu\leqslant 1/\sqrt{2}$ for the interior scheme when the standard five-point stencil for (2.1) is used:

$$u_{n+1k}^j-2u_{nk}^j+u_{n-1k}^j$$
$$=\mu^2\{u_{nk}^{j+1}-4u_{nk}^j+u_{nk}^{j-1}+u_{nk+1}^j+u_{nk-1}^j\}. \tag{2.11}$$

We are now assuming a square grid $\Delta x=\Delta y$, as this simplifies the analysis to the point where it is manageable.

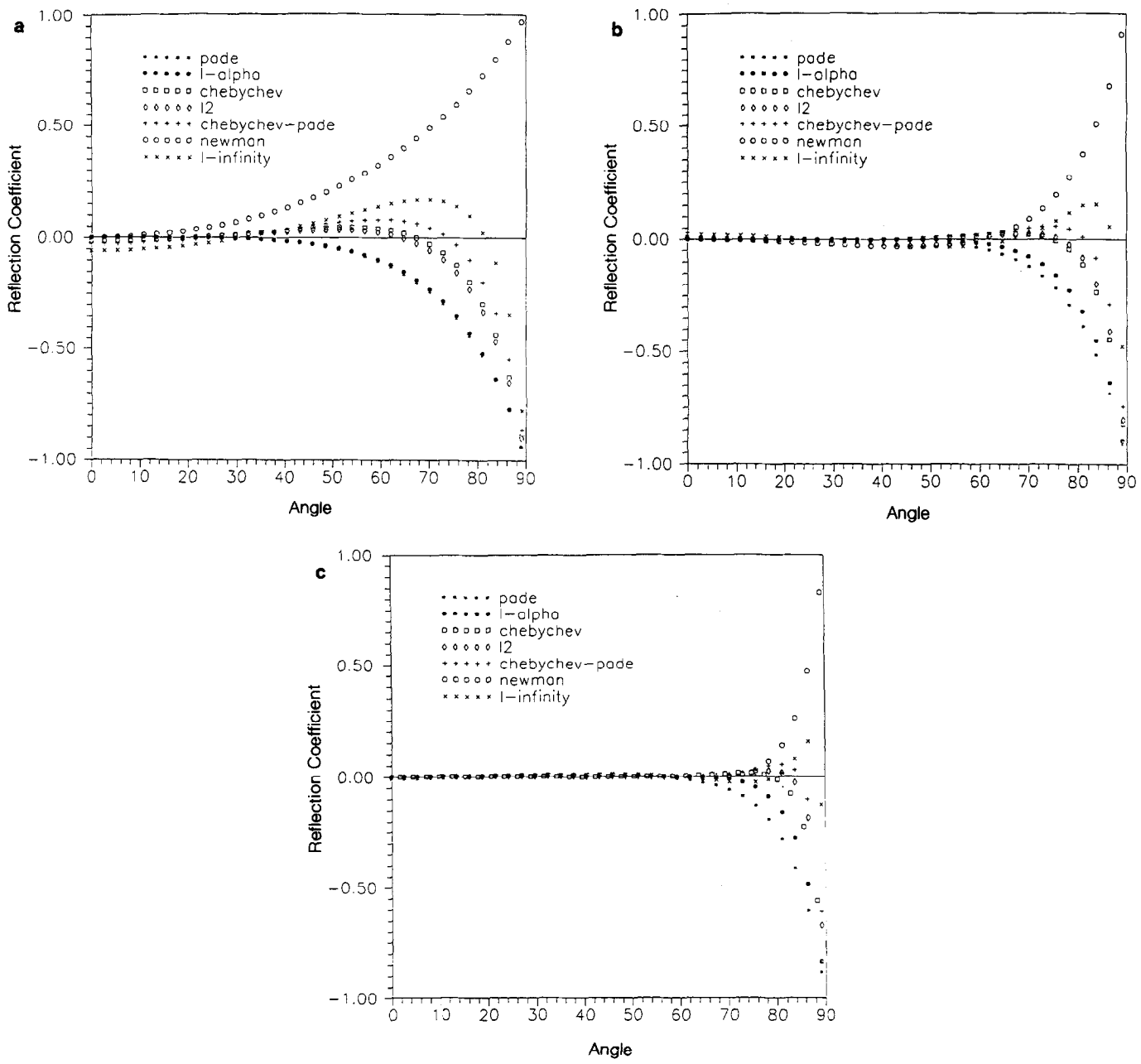

FIG. 1. (a) Reflection coefficients for $k = 2$. (b) Reflection coefficients for $k = 3$. (c) Reflection coefficients for $k = 4$.

From Fig. 1a it is apparent that the least squares, Chebyshev–Padé, and Chebyshev approximations give the least reflection over a wide range of angles. The bound $\mu < -1/2p_2$, however, reduces the effectiveness of the equation. This may be overcome by using an alternative operator. Another discretization which is also second order in space and time is given by

$$D_+^x D_0^t u_{nk}^0 - \frac{p_0}{2c} D_+^t D_-^t (u_{nk}^0 + u_{nk}^1) - \frac{p_2 c}{2} D_+^y D_-^y (u_{nk}^0 + u_{nk}^1) = 0. \tag{2.12}$$

Observe that this operator is symmetric in time, whereas (2.10) is not. We shall see that operators which are symmetric in time prove to have less restrictive bounds on μ. The stencils are given in Fig. 2.

Buneman [0] has also used Eq. (2.12). There are many other ways to discretize (2.9); for example, we could use a first-order operator:

$$D_+^x D_0^t u_{nk}^0 - \frac{p_0}{c} D_+^t D_-^t u_{nk}^0 - p_2 c D_+^y D_-^y u_{nk}^0 = 0. \tag{2.13}$$

We prove in Section 5 that (2.12) and (2.13) are stable only

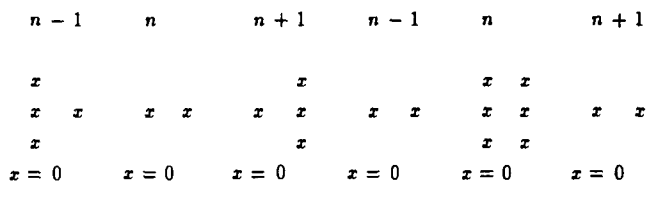

(2.10) (2.12)

FIG. 2. Stencils for Eqs. (2.10) and (2.12).

if $\mu < \sqrt{p_0/|p_2|}$. These bounds are given in Table II. Observe that the bound on (2.12) is less restrictive than the von Neumann bound in all cases. In Section 6 we present numerical comparisons of these methods.

The $k=3$ and $k=4$ equations have smaller reflection coefficients and thus we compare these equations with the $k=2$ equations as well. To derive discretizations for $k=3$ and $k=4$ we attempted to use the same ideas as for (2.12). We used central differencing for the second-order derivatives, a forward difference for the spatial first-order derivatives and a backward difference for the first-order time derivatives. To get a truncation error of $O(\Delta x^2)+O(\Delta t^2)+O(\Delta x\,\Delta t)$ we then averaged over space and time. For the $k=3$ equation,

$$cu_{ttx}+c^3q_2u_{yyx}=p_0u_{ttt}+c^2p_2u_{yyt}, \tag{2.14}$$

we have the operator

$$\begin{aligned}&\frac{1}{2}cD_+^tD_-^tD_+^x(u_{nk}^0+u_{n-1k}^0)\\&+c^3\frac{q_2}{2}D_+^yD_-^yD_+^x(u_{nk}^0+u_{n-1k}^0)\\&-\frac{p_0}{2}D_+^t(D_-^t)^2(u_{nk}^0+u_{nk}^1)\\&-c^2\frac{p_2}{2}D_+^yD_-^yD_-^t(u_{nk}^0+u_{nk}^1)=0.\end{aligned} \tag{2.15}$$

For the $k=4$ equation,

$$cu_{tttx}+q_2c^3u_{yytx}=p_0u_{tttt}+p_2c^2u_{yytt}+p_4c^4u_{yyyy}, \tag{2.16}$$

TABLE II

Theoretical Bounds on Courant Number μ

Approximation	Padé	L_α^∞	Chebyshev points	L^2	C-P	Newman points	L^∞
Method 2.10							
$-\frac{1}{2p_2}$	1.0	0.9698	0.6533	0.6791	0.5890	0.5000	0.5000
Methods 2.12 *and* 2.13							
$\sqrt{p_0/\lvert p_2\rvert}$	1.414	1.3929	1.1634	1.1832	1.1180	1.0000	1.0607
Method 2.15							
$\sqrt{p_0/\lvert p_2\rvert}$	1.1547	1.1119	1.0448	1.0373	1.0247	1.0000	1.0068
$\sqrt{p_0/(p_0q_2-p_2)}$	1.4142	1.4254	1.5041	1.5517	1.5952	1.7401	1.9234
Method 2.17							
$\left(\frac{1}{2p_4}(p_2+\sqrt{p_2^2+4p_0p_4})\right)^{1/2}$	1.3409	1.2257	1.1657	1.1652	1.1160	1.0650	1.0334
$\left(\frac{1}{4p_4}(p_2-p_0q_2+\sqrt{(p_0q_2-p_2)^2+8p_0p_4})\right)^{1/2}$	1.1118	1.0173	0.9685	0.9209	0.9225	0.8724	0.8385
Method 4.10							
$\sqrt{p_0/(p_0q_2-p_2)}$	1.4142	1.4086	1.4001	1.3687	1.3743	1.3209	1.2643
$\left(\frac{-p_2-\sqrt{p_2^2-4p_0p_4}}{2p_4}\right)^{1/2}$	1.0824	1.0416	1.0195	1.0108	1.0084	1.0000	1.0012
$\left(\frac{(p_2-p_0q_2)p_0}{p_0p_4+p_2(p_0q_2-p_2)}\right)^{1/2}$	1.1547	1.1775	1.2047	1.2363	1.2380	1.2526	1.2327

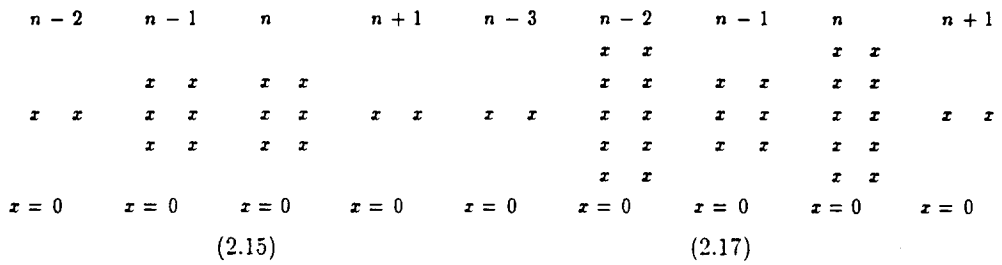

FIG. 3. Stencils for Eqs. (2.15) and (2.17).

the operator is

$$\frac{c}{2} D^t_+ (D^t_-)^2 D^x_+ (u^0_{nk} + u^0_{n-1k})$$

$$+ \frac{q_2}{2} c^3 D^y_- D^y_+ D^t_- D^x_+ (u^0_{nk} + u^0_{n-1k})$$

$$- \frac{p_0}{2} D^t_+ (D^t_-)^3 (u^0_{nk} + u^1_{nk})$$

$$- p_2 \frac{c^2}{2} D^y_- D^y_+ (D^t_-)^2 (u^0_{nk} + u^1_{nk})$$

$$- p_4 \frac{c^4}{4} (D^y_- D^y_+)^2$$

$$\times (u^0_{nk} + u^1_{nk} + u^0_{n-2k} + u^1_{n-2k}) = 0. \qquad (2.17)$$

These stencils are illustrated in Fig. 3.

Contrary to Higdon's conjecture [8], we have found explicit schemes not only for $k = 3$ equations but also for $k = 4$ equations. Because of the increased order of the time derivative as k increases, extra time levels need to be stored at the boundary. The derivation of Eqs. (2.15) and (2.17) is tedious and the extension to $k = 5$ daunting. In Section 4 we show how to avoid this problem.

As for (2.10), (2.12), and (2.13) we have investigated the stability of (2.15) and (2.17). The bounds on μ for stability are reviewed in Table II. Note that all of the results pertain to the interior equation solved by (2.11), the five-point difference stencil. The relevance of these results to other interior schemes is discussed in Renaut [17].

3. HIGDON'S OPERATORS

Higdon [10] introduced absorbing boundary conditions of the form

$$\left[\prod_{j=1}^{p} \left(\cos \alpha_j \frac{\partial}{\partial t} - c \frac{\partial}{\partial x} \right) \right] u = 0, \qquad (3.1)$$

where $|\alpha_j| < \pi/2$ for all j. This equation is satisfied exactly by any linear combination of plane waves travelling across $x = 0$ at angles of incidence $\pm\alpha_1, \pm\alpha_2, ..., \pm\alpha_p$ with speed c. The reflection coefficient for (3.1) is given by

$$R = \prod_{j=1}^{p} \left(\frac{\cos \alpha_j - \cos \theta}{\cos \alpha_j + \cos \theta} \right). \qquad (3.2)$$

Therefore the angles α_j can be chosen to distribute the zeros of R and thus optimize the absorption properties of (3.1). In this paper we choose the angles α_j to match the interpolating angles of the absorbing boundary conditions in Section 2 as given in Table 5 of Halpern and Trefethen [4]. As shown by Higdon [10] and Halpern and Trefethen [6] this gives methods with identical reflection coefficients. They are thus equivalent but are implemented differently. In fact we can go from any of the schemes described by (2.6) to Eq. (3.1) by replacing the second-order derivatives in y through $u_{yy} = (1/c^2) u_{tt} - u_{xx}$. In Section 6 we compare these equations numerically.

Higdon [10] suggests the first-order approximation

$$\cos \alpha_j D^t_- (1 + a \, \Delta x \, D^x_+) u^0_{n+1k}$$
$$- c D^x_+ [1 - b \, \Delta t \, D^t_-] u^0_{n+1k} = 0 \qquad (3.3)$$

for each of the factors in (3.1). In one series of experiments the amount of reflected energy was minimal for $a = b = 0.25$. Observe, however, that $a = b = 0.5$ gives a second-order approximation to a factor of (3.1). We present results using both choices for $a = b$. According to Theorem 2, Higdon [10] the operator (3.3) is stable if $a \leqslant \frac{1}{2}$ when $a = b$, and there is no further restriction on μ provided that the interior scheme is stable. Note also that he further observes that this restriction $a \leqslant \frac{1}{2}$ can be relaxed slightly when $\mu < 1/\sqrt{2}$ [10].

4. LINDMAN'S BOUNDARY CONDITION

Lindman [14] is apparently the first person who considered solving the absorbing boundary problem by the use of an approximation to the one-way wave equation at the boundary. Instead of approximating the square root in

Eq. (2.4) he looked for an approximation to the inverse square root

$$R(s)=\frac{A_m(s)}{D_n(s)}=\frac{1}{\sqrt{1-s^2}}. \tag{4.1}$$

Here $R(s)$ is constrained, however, to be of the form

$$R(s)=1+\sum_{i=1}^{N}\frac{\alpha_i s^2}{1-\beta_i s^2} \tag{4.2}$$

which means that $a_0=d_0=1$, and $D_n(s)=\prod_{i=1}^{N}(1-\beta_i s^2)$. For general approximations $R(s)$, we obtain a partial differential equation

$$\sum_{i=0}^{m} a_i c^{i+1} u_{y^i t^K - i_x} = \sum_{i=0}^{n} d_i c^i u_{y^i t^{K-i+1}}, \tag{4.3}$$

where $K=\max\{m, n-1\}$. If none of the β_i or α_i are zero, $m=n=2N$. Clearly Eq. (4.3) is the analogue of (2.7) in Section 2. Thus Lindman's method corresponds to the solution of (4.3) for $m=n=6$, where

$$\begin{aligned}
&a_0=1, \qquad a_2=\sum_{i=1}^{3}(\alpha_i-\beta_i)\\
&a_4=\beta_1\beta_2+\beta_3\beta_2+\beta_3\beta_1-\alpha_1(\beta_2+\beta_3)\\
&\qquad -\alpha_2(\beta_1+\beta_3)-\alpha_3(\beta_1+\beta_2),\\
&a_6=\alpha_1\beta_2\beta_3+\alpha_2\beta_1\beta_3+\alpha_3\beta_2\beta_1-\beta_1\beta_2\beta_3,\\
&d_2=-(\beta_1+\beta_2+\beta_3),\\
&d_4=\beta_1\beta_2+\beta_3\beta_1+\beta_3\beta_2,\\
&d_6=-\beta_1\beta_2\beta_3.
\end{aligned}$$

Observe also that by uniqueness, the Padé approximations (4.1) satisfy $A_m(s)=Q_n(s)$ and $D_n(s)=P_m(s)$, where $Q_n(s)$ and $P_m(s)$ are the polynomials of $r(s)$ in Eq. (2.6).

Lindman does not use (4.3) as the boundary condition. Instead he makes use of the term (4.2). If we insert (4.2) into the dispersion relation (2.4) we obtain

$$i(\omega-\xi c)=i\left(\xi c\sum_{j=1}^{N}\frac{\alpha_j s^2}{1-\beta_j s^2}\right). \tag{4.4}$$

Then, associating $i\omega$, $i\xi$, and $i\eta$ with partial differentiation by t, x, and y, respectively, in the usual way, we obtain

$$u_t-cu_x=c\sum_{i=1}^{N}h_i, \tag{4.5}$$

where

$$\frac{\partial^2 h_i}{\partial t^2}-\beta_i c^2\frac{\partial^2 h_i}{\partial y^2}=\alpha_i c^2\frac{\partial^2}{\partial y^2}\left(\frac{\partial u}{\partial x}\right).$$

Therefore, instead of solving (4.3) directly, Lindman solves a system of $N+1$ equations at the boundary. The first of these is the normal incidence-absorbing boundary condition modified by the correction functions h_i. These correction functions are the solutions of one-dimensional wave equations along the boundary.

Since Eqs. (4.3) and (2.7) are similar we can use Lindman's approach for the solution of the equations in Section 2. The rational function $r(s)$ to the square root can be expressed in a Lindman form

$$r(s)=p_0\left(1+\sum_{i=1}^{N}\frac{\alpha_i s^2}{1-\beta_i s^2}\right), \tag{4.6}$$

where $2N=\max\{m, n\}$. Thus we can use this form in the dispersion relation (2.4) to give the system of equations

$$u_x-\frac{p_0}{c}u_t=\frac{p_0}{c}\sum_{i=1}^{N}h_i,$$

where

$$\frac{\partial^2 h_i}{\partial t^2}-\beta_i c^2\frac{\partial^2 h_i}{\partial y^2}=c^2\alpha_i\frac{\partial^3 u}{\partial y^2\,\partial t}, \qquad i=1, \ldots, N, \tag{4.7}$$

that must be solved at the boundary.

Equipped with this new formulation, it is much easier to find a difference approximation for Eqs. (4.3). Lindman solved the system (4.5) with the discrete approximation

$$D_+^t\frac{(u_{nk}^0+u_{nk}^1)}{2}-cD_+^x\frac{(u_{n+1k}^0+u_{nk}^0)}{2}=c\sum_{i=1}^{N}(h_i)_{nk}^0 \tag{4.8}$$

and

$$\begin{aligned}
&(D_+^t D_-^t-\beta_i c^2 D_+^y D_-^y)(h_i)_{n-1k}^0\\
&\qquad=\alpha_i\frac{c^2}{2}(D_+^y D_-^y)\,D_+^x(u_{nk}^0+u_{n-1k}^0),
\end{aligned}$$

where $(h_i)_{nk}^0$ is an approximation to $h_i(0, k\,\Delta y, n\,\Delta t)$. The second-order derivatives are approximated by a second-order central difference and the first-order derivatives by forward differences averaged over two levels. The equation for the h_i has a truncation error $O(\Delta x)+O(\Delta t)$. In Section 6 we see that this does not degrade the results.

Therefore, we apply an equivalent difference scheme for Eqs. (4.7):

$$\begin{aligned} &cD_+^x(u_{n+1k}^0+u_{nk}^0)-p_0D_+^t(u_{nk}^0+u_{nk}^1)\\ &\quad=p_0\sum_{i=1}^{N}(h_i)_{nk}^0,\\ &(D_+^tD_-^t-\beta_ic^2D_+^yD_-^y)(h_i)_{n-1k}^0\\ &\quad=\alpha_iD_+^yD_-^yD_+^tc^2(u_{n-1k}^1+u_{n-1k}^0). \end{aligned} \tag{4.9}$$

For the $k=2$ equation, $r(s)=p_0+p_2s^2$, Eqs. (4.9) give the same difference operator as (2.12), where $\alpha_1=p_2/p_0$ and $\beta_1=0$. The $k=3$ equation also gives the operator (2.15), where $\alpha_1=p_2/p_0-q_2$ and $\beta_1=-q_2$. For $k=4$, however, (4.9) leads to

$$\begin{aligned} &D_+^t(D_-^t)^2D_+^x(u_{nk}^0+u_{n-1k}^0)\\ &\quad+q_2c^3D_-^yD_+^yD_-^tD_+^x(u_{nk}^0+u_{n-1k}^0)\\ &\quad-p_0D_+^t(D_-^t)^3(u_{nk}^0+u_{nk}^1)\\ &\quad-p_2c^2D_-^yD_+^y(D_-^t)^2(u_{nk}^0+u_{nk}^1)\\ &\quad-p_4(D_+^yD_-^y)^2(u_{n-1k}^0+u_{n-1k}^1)=0 \end{aligned} \tag{4.10}$$

which differs from (2.17) in the last term. The stencil for (4.10) is illustrated in Fig. 4 and may be compared with that for (2.17) in Fig. 3. We prove in Section 5 that (4.10) and (2.17) may be stable but the results in Section 6 demonstrate that (4.10) is superior.

We stress that we do not suggest that Eqs. (4.9) be expanded and solved in the format of Section 2. For the sake of comparison we eliminated the variables h. It is, however, much easier to program (4.9) for $k=4$ than (4.10). The form of (4.9) makes the use of higher order approximations, i.e., larger k, a simple change that means incrementing a loop index rather than a completely new subroutine. It is not difficult to find the coefficients $\{\alpha_i, \beta_i, i=1, ..., N\}$ from the polynomial coefficients when m and n are small, as considered here.

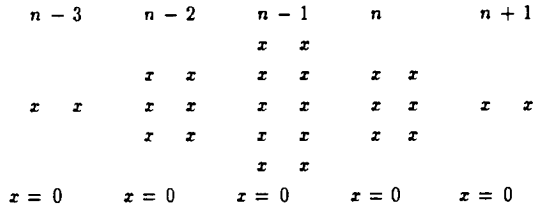

Fig. 4. Stencil for (4.10).

5. STABILITY

To find necessary conditions for stability for any boundary operator we use the Gustafsson, Kreiss, and Sundström [5] theory in the form explained by Higdon [8, 10]. Any of the boundary conditions considered here can be expressed in a operator format

$$B(K, Y, Z^{-1})\,u_{n+1k}^0=0,$$

where B is a polynomial in the three variables K, Y, and Z which denote the forward shift operators with respect to x, y, and t, respectively. We use the stability criterion

$$B(\kappa, y, z^{-1})\neq 0 \qquad \text{whenever} \quad |z|\geqslant 1,\ |\kappa|\leqslant 1,$$

explained in Higdon [8, 10]. Physical interpretation of this condition is given by Higdon [8, 10] and Trefethen [21, 22] and amounts to requiring that the boundary does not support waves which travel into the domain and are supported by the interior scheme.

To find bounds on the Courant number for which a method may be stable we use the same approach as Renaut and Petersen [16]. This involves writing the operator B as a polynomial in z^{-1} and finding conditions for which there are no roots satisfying $|\kappa|<1$ and $|z|\geqslant 1$. To do this we use the theory of Schur transforms as described by Henrici [7]. Let $p(z)$ be a polynomial of degree n,

$$p(z):=a_nz^n+a_{n-1}z^{n-1}+\cdots+a_0.$$

Define the reciprocal polynomial of p by p^*,

$$p^*(z)=\bar{a}_0z^n+\bar{a}_1z^{n-1}+\cdots+\bar{a}_n.$$

The polynomial T_p defined by

$$Tp(z):=\bar{a}_0\,p(z)-a_n\,p^*(z)$$

is of degree $n-1$ and is called the Schur transform of p. Furthermore,

$$Tp(0)=|a_0|^2-|a_n|^2$$

is always real. We can repeat the process to find the Schur transform of Tp, T^2p. Note that the Schur transform of a polynomial of degree zero is the zero polynomial. Thus we have the iterated Schur transforms T^kp defined by

$$T^kp:=T(T^{k-1}p), \qquad k=2, 3, ..., n,$$

and we can set $\gamma_k:=T^kp(0)$, $k=1, 2, ..., n$. Then quoting from Henrici [7] we have conditions on the γ_k for the zeros of p to lie outside the unit circle:

THEOREM 6.8(b) (Henrici [7]). *Let p be a polynomial*

of degree n, $p \neq 0$. All zeros of p lie outside the unit disk $|z| \leqslant 1$ if and only if $\gamma_k > 0$, $k = 1, 2, ..., n$.

Considering B as a polynomial in $W = z^{-1}$ we obtain conditions for the zeros to satisfy $|W| > 1$ and thus $|z| < 1$, provided that $|\kappa| < 1$. When $|\kappa| = 1$ there can be no solutions of both the interior and the boundary operator which have $|z| > 1$, see Higdon [10]. Roots with $|\kappa| = |z| = 1$, however, may exist and need to be considered. Higdon [10] showed that the wavelike solutions of (2.11) which have group velocity in the x-direction greater than zero and hence correspond to waves pointing into the domain satisfy $\arg \kappa \arg z < 0$. Therefore we need to determine whether these solutions, called generalised eigensolutions of the second kind, also satisfy the boundary condition. Physically these solutions correspond to waves radiating spontaneously from the boundary into the interior. The GKS theory also does not allow solutions for which the group velocity is zero in the x-direction, generalised eigensolutions of the first kind. These correspond to waves travelling up and down the boundary. In practice, however, we need to distinguish between the generalised eigensolutions of the first kind and of the second kind (cf. Kreiss [13] and Higdon [9]). Trefethen [22] demonstrated that linear growth due to generalised eigensolutions of the second kind at one boundary is converted to exponential growth by repeated reflection at a second boundary. Instability due to eigensolutions of the first kind has not been widely observed. Higdon [8] reported incompatibility between initial and boundary data as a mechanism that might excite instability in the case of zero frequency generalized eigensolutions. In [10] he reports how this zero frequency problem can be removed by adding positive constants to the boundary operator. Renaut and Petersen [16] also observed instability due to incompatibility. Their experiments are repeated in Section 6 with the incompatibility removed and the instability is not excited.

To analyse stability we consider waves that are oscillatory in y, so $y = e^{i\eta \Delta y}$. Modes of the form $\kappa^j e^{i\eta y} z^n$ are used in the stability theory because they arise from using a Fourier transform in the direction of the boundary and a Laplace transform in time.

We now quote the results for each of the schemes considered in Section 2. These results are based on some assumptions about the coefficients of the approximations. We believe these assumptions are justified because they hold in all cases considered here. The proofs are given later in this section.

THEOREM 5.1. *The difference schemes given by Eq. (2.12) are stable in combination with Eq. (2.11) only if*

$$\mu < \sqrt{p_0/|p_2|}, \qquad \eta \Delta y \neq 0,$$

assuming that $p_0 > 0$ and $p_2 < 0$.

THEOREM 5.2. *The difference schemes given by Eq. (2.13) are stable in combination with Eq. (2.11) only if*

$$\mu < \sqrt{p_0/|p_2|}, \qquad \eta \Delta y \neq 0,$$

assuming that $p_0 > 0$ and $p_2 < 0$.

THEOREM 5.3. *The difference schemes given by Eq. (2.15) are stable in combination with Eq. (2.11) only if*

$$\mu < \min\{\sqrt{p_0/|p_2|}, \sqrt{p_0/(p_0 q_2 - p_1)}\}, \qquad \eta \Delta y \neq 0,$$

provided that $p_2 - p_0 q_2 < 0$, $p_0 > 0$, $q_2 < 0$, and $p_2 < 0$.

THEOREM 5.4. *The difference schemes given by Eq. (2.17) are stable in combination with Eq. (2.11) only if*

$$\mu^2 < \min\left\{\frac{1}{p_4}(p_2 + \sqrt{p_2^2 + 4p_0 p_4}),\ \frac{1}{4p_4}(p_2 - p_0 q_2 + \sqrt{(p_0 q_2 - p_2)^2 + 8p_0 p_4})\right\}, \quad \eta \Delta y \neq 0,$$

provided that $p_0 q_2 - p_2 > 0$, $p_0 > 0$, $p_2 < 0$, $p_4 > 0$, $q_2 < 0$, and $p_4 + q_2(p_0 q_2 - p_2) < 0$.

THEOREM 5.5. *The difference schemes given by Eq. (4.10) are stable in combination with Eq. (2.11) only if*

$$\mu^2 < \min\left\{\frac{p_0}{p_0 q_2 - p_2}, \frac{-p_2 - \sqrt{p_2^2 - 4p_0 p_4}}{2p_4}, \frac{(p_2 - p_0 q_2) p_0}{p_0 p_4 + p_2(p_0 q_2 - p_2)}\right\}, \qquad \eta \Delta y \neq 0,$$

provided that the conditions of Theorem 5.4. hold.

The results of these theorems are summarized in Table II. Of course the bounds given in Table II are the maximum Courant numbers for which the boundary conditions can be stable. In those cases where this bound is larger than $1/\sqrt{2}$, which is the bound on μ for the interior scheme, the largest μ that may be stably used is $1/\sqrt{2}$. We show separately that in every case except (5.2) generalised eigensolutions may exist and that if they exist the reflection coefficient is less than one. In Table III we give the numerical stability conditions for comparison. Except for (5.4) these bounds are accurately predicted by the theoretical results.

Proof of Theorem 5.1. For (2.12) the operator B is

$$B = \frac{(\kappa - 1)(1 - z^{-2})}{2\Delta t\, \Delta x} - \frac{p_0}{2c}\frac{(1 - 2z^{-1} + z^{-2})(1 + \kappa)}{\Delta t^2} - \frac{p_2 c}{2}\left(\frac{y - 2 + y^{-1}}{\Delta y^2}\right)(1 + \kappa)\, z^{-1}.$$

Let $b = p_2\mu$ and $a = p_0/\mu$; then we have an operator quadratic in $W = z^{-1}$,

$$B(\kappa, W) = R(\kappa) + S(\kappa)W + P(\kappa)W^2,$$

where

$$R(\kappa) = \kappa - 1 - a(1+\kappa)$$
$$S(\kappa) = 2(a - \tilde{b})(1+\kappa)$$
$$P(\kappa) = -[\kappa - 1 + a(1+\kappa)].$$

To simplify the algebra we have replaced $b(\cos \eta\, \Delta y - 1)$ by $\tilde{b}$. The iterated Schur transforms of B give

$$\gamma_1 = |R|^2 - |P|^2$$
$$\gamma_2 = (|R|^2 - |P|^2)^2 - (|\bar{R}S - P\bar{S}|)^2.$$

It can be shown that $\gamma_1 = -4a(|\kappa|^2 - 1) > 0$ for $|\kappa| < 1$, provided that $p_0 > 0$. Since

$$\bar{R}S - P\bar{S} = 4(a - \tilde{b})(|\kappa|^2 - 1),$$
$$\gamma_2 = 16(|\kappa|^2 - 1)^2\, \tilde{b}(2a - \tilde{b}).$$

For $\eta\, \Delta y \neq 0$, $\tilde{b} > 0$, provided that $p_2 < 0$. Thus $\gamma_2 > 0$ if $2a - \tilde{b} > 0$, which gives the condition $\mu < \sqrt{p_0/|p_2|}$.

When $\eta\, \Delta y = 0$ a pair (κ, z), which is a solution at the boundary and the interior, satisfies

$$B(\kappa, z^{-1}) = (\kappa - 1)(z - z^{-1}) - \frac{p_0}{\mu}(1+\kappa)(z - 2 + z^{-1}) = 0$$

and

$$z - 2 + z^{-1} = \mu^2(\kappa - 2 + \kappa^{-1}).$$

Thus

$$(\kappa - 1)(1 - z^{-2}) - p_0\mu(1+\kappa)(\kappa - 1)(1 - \kappa^{-1})\, z^{-1} = 0$$

and the pair $(1, 1)$ is a solution. Therefore $B(1, 1) = 0$ and thus the boundary condition has a generalized eigensolution at frequency and wavenumber zero and the stability condition is violated. Higdon [8], however, has shown that this solution is inevitable and does not cause a significant problem unless there are incompatibilities between the initial and boundary data. Otherwise, a pair (κ, z) which is a root of both equations is complex with $|\kappa| = |z| = 1$ or $z = -1$ and κ is real, $\kappa < 0$. In either case κ and z have arguments of the same sign and so do not lead to instability. ∎

Proof of Theorem 5.2. For (2.13) the operator B is given by

$$B = (\kappa - 1)(z - z^{-1}) - 2a(z - 2 + z^{-1}) - 2b(y - 2 + y^{-1}),$$

where $a = p_0/\mu$ and $b = p_2\mu$. This is a quadratic equation as in Theorem 5.1 and we find that for stability we need

$$16(\bar{\kappa} + \kappa - 2)^2\, \tilde{b}(2a - \tilde{b}) > 0$$

which again gives $\mu^2 < p_0/|p_2|$ for $\eta\, \Delta y \neq 0$.

For $\eta\, \Delta y = 0$ the pairs (κ, z) are real and are either both inside the unit circle or both outside the unit circle, unless $\kappa = z = 1$. ∎

Proof of Theorem 5.3. For (2.15) the operator $B(\kappa, y, z^{-1})$ leads to a cubic in $W = z^{-1}$,

$$B(W) = R(\kappa) + S(\kappa)W + T(\kappa)W^2 + P(\kappa)W^3,$$

where

$$R = \kappa - 1 - a(1+\kappa)$$
$$S = -(\kappa - 1) + b(\kappa - 1) + 3a(1+\kappa) - c(1+\kappa)$$
$$T = -(\kappa - 1) + b(\kappa - 1) - 3a(1+\kappa) + c(1+\kappa)$$
$$P = \kappa - 1 + a(1+\kappa)$$

and $a = p_0/\mu$, $b = q_2\mu^2(y - 2 + y^{-1})$, and $c = p_2\mu(y - 2 + y^{-1})$. The first Schur transform of B is

$$T(B) = |R|^2 - |P|^2 + W(\bar{R}S - P\bar{T}) + W^2(\bar{R}T - P\bar{S}).$$

Therefore, $\gamma_1 = |R|^2 - |P|^2$ and, as in Theorem 5.1, $\gamma_1 = -4a(|\kappa|^2 - 1) > 0$, provided $\kappa < 1$ and $p_0 > 0$. The analysis is simplified if we calculate the coefficients of $T(B)$ before finding the next Schur iterate. Now

$$\bar{R}S - P\bar{T} = 2(|\kappa|^2 - 1)(4a - c - ab)$$

and

$$\bar{R}T - P\bar{S} = 2(|\kappa|^2 - 1)(-2a + c - ab).$$

Thus

$$T(B) = 2(|\kappa|^2 - 1)(-2a + W(4a - c - ab) + W^2(-2a + c - ab))$$

has real coefficients. Let $B_1(W)$ be $T(B)/2(|\kappa|^2 - 1)$ and defined by

$$B_1 = -2a + eW + fW^2,$$

where $e=4a-c-ab$ and $f=-2a+c-ab$. Then B_1 is Schur, provided that

$$\gamma_2=4a^2-f^2>0$$

and $\gamma_3=(4a^2-f^2)^2-(-2a-f)^2e^2>0$. Now γ_2 factors to give $\gamma_2=(4a-c+ab)(c-ab)$. Substituting the values of a, b, and c, we have

$$\gamma_2=2\mu(\cos\eta\,\Delta y-1)(p_2-p_0q_2)\times\left(\frac{4p_0}{\mu}-2\mu(\cos\eta\,\Delta y-1)(p_2-p_0q_2)\right).$$

Then, provided that $p_2-p_0q_2<0$, we require

$$2p_0-\mu^2(\cos\eta\,\Delta y-1)(p_2-p_0q_2)>0$$

which leads to the condition

$$\mu<\sqrt{p_0/(p_0q_2-p_2)}.$$

Simplifying γ_3 we have

$$\gamma_3=(2a-f-e)(2a-f+e)$$

which after substitution is

$$\gamma_3=16p_0q_2(\cos\eta\,\Delta y-1)(2p_0-p_2\mu^2(\cos\eta\,\Delta y-1)).$$

Thus $\gamma_3>0$ for $\eta\,\Delta y\neq 0$, provided that $\mu^2<p_0/|p_2|$ and $p_2<0$ and $q_2<0$.

The solutions with $\eta\,\Delta y=0$ are exactly the same as those in Theorem 5.1 and do not lead to instability. ▮

Proof of Theorem 5.4. For (2.17) we obtain an operator quartic in $W=z^{-1}$,

$$B(W)=R+SW+TW^2+PW^3+QW^4,$$

where

$$R=\kappa-1+a(1+\kappa),$$
$$S=(c-2)(\kappa-1)+(b+d-4a)(1+\kappa)$$
$$T=(6a-2b)(1+\kappa)$$
$$P=(2-c)(\kappa-1)+(b+d-4a)(1+\kappa)$$
$$Q=a(1+\kappa)-(\kappa-1),$$

and $a=-p_0/\mu$, $b=-p_2\mu(y-2+y^{-1})$, $c=q_2\mu^2(y-2+y^{-1})$, and $d=-(p_4\mu^3/2)(y-2+y^{-1})^2$.

The first Schur transform is

$$T(B)=|R|^2-|Q|^2+(\bar RS-Q\bar P)W+(\bar RT-Q\bar T)W^2+(\bar RP-Q\bar S)W^3.$$

Again $\gamma_1=4a(|\kappa|^2-1)>0$ for $p_0>0$ and $|\kappa|<1$. The coefficients of $T(B)$ are

$$\bar RS-Q\bar P=2(|\kappa|^2-1)(ac-6a+b+d)$$
$$\bar RT-Q\bar T=2(6a-2b)(|\kappa|^2-1)$$

and

$$\bar RP-Q\bar S=2(|\kappa|^2-1)(b+d-2a-ac)$$

which are again real. Thus we find the Schur iterates of $B_1(W)=T(B)/2(|\kappa|^2-1)$ defined by

$$B_1(W)=X+YW+ZW^2+VW^3,$$

where $X=2a$, $Y=ac-6a+b+d$, $Z=6a-2b$, and $V=b+d-2a-ac$. Therefore,

$$T(B_1)=X^2-V^2+(XY-VZ)W+(XZ-VY)W^2$$

and $\gamma_2=X^2-V^2=(4a+ac-b-d)(b+d-ac)$. Now

$$(b+d-ac)=2(\cos\eta\,\Delta y-1)\times\mu[p_0q_2-p_2-p_4\mu^2(\cos\eta\,\Delta y-1)]<0,$$

provided that $p_0q_2-p_2>0$ and $p_4>0$. We therefore need $4a+ac-b-d<0$ for stability. This means that the polynomial in $x=\mu\sin(\eta\,\Delta y/2)$,

$$f(x)=x^4+\left(\frac{p_0q_2-p_2}{p_4}\right)x^2-\frac{p_0}{2p_4},$$

should be negative. This is the case, provided that

$$\mu^2<\frac{1}{4p_4}[p_2-p_0q_2+\sqrt{(p_0q_2-p_2)^2+8p_0p_4}].$$

Now

$$\gamma_3=(X^2-V^2)^2-(XZ-VY)^2=-4a((b+d)(c-2)+2b-ac^2)\times((b+d-4a)(b+d-ac)-2ad).$$

The factor $(b+d)(c-2)+2b-ac^2$

$$=4\mu^3(\cos\eta\,\Delta y-1)^2[q_2(p_0q_2-p_2)+p_4-q_2p_4\mu^2(\cos\eta\,\Delta y-1)]<0,$$

provided that $p_4+q_2(p_0q_2-p_2)<0$. Then for $\gamma_3>0$ we need $(b+d-4a)(b+d-ac)-2ad<0$, which means that we should have, at least, that $(b+d-4a)>0$, as the other terms are negative, hence the condition

$$\mu^2<\frac{1}{4p_4}[p_2+\sqrt{p_2^2+8p_0p_4}].$$

The expression for $\gamma_4=(X^2-V^2-XZ+VY)^2(X^2-V^2)(X+V+Y+Z)(X-V+Z-Y)$ simplifies to the condition

$$4d(8a-2b-d)>0.$$

Since $d<0$, $8a-2b-d<0$ is required, which is the case for $\mu^2<(1/p_4)[p_2+\sqrt{p_2^2+4p_0p_4}]$. Observe that this bound on μ is larger than the bound given for γ_3 and thus $\gamma_4>0$, provided that $\gamma_3>0$.

In the above we have assumed that $\eta\,\Delta y\neq 0$. When $\eta\,\Delta y=0$,

$$B=(1-z^{-1})^3[(\kappa-1)(1+z^{-1})+a(\kappa+1)(1-z^{-1})].$$

Therefore the pair $(\kappa, z)=(1, 1)$ is a solution and the other solutions satisfy $(z+1)/(z-1)=-a(\kappa+1)/(\kappa-1)$. The maps $-a(\kappa+1)/(\kappa-1)$ and $(z+1)/(z-1)$ take the unit circle to the imaginary axis with its interior going to the left-half plane and its exterior to the right-half plane. Therefore, the only other pairs (κ, z) which are solutions have either both $|\kappa|$ and $|z|>1$ or both $|\kappa|$ and $|z|<1$. ∎

Proof of Theorem 5.5. As in (5.4) Eq. (4.10) gives an operator quartic in W,

$$B(W)=R+SW+TW^2+PW^3+QW^4,$$

where

$$\begin{aligned}R&=\kappa-1+a(1+\kappa)\\S&=(b-4a)(1+\kappa)+(c-2)(\kappa-1)\\T&=(6a-2b+d)(\kappa+1)\\P&=(b-4a)(1+\kappa)-(c-2)(\kappa-1)\\Q&=a(1+\kappa)-(\kappa-1)\end{aligned}$$

and a, b, c are defined as in (5.4) but $d=-p_4\mu^3(y-2+y^{-1})^2$. As in (5.4), $\gamma_1=|R|^2-|Q|^2>0$, provided $p_0>0$. The coefficients of $T(B)$ are

$$\begin{aligned}\bar{R}S-Q\bar{P}&=2(b-6a+ac)(|\kappa|^2-1)\\\bar{R}T-Q\bar{T}&=2(6a-2b+d)(|\kappa|^2-1)\\\bar{R}P-Q\bar{S}&=2(b-2a-ac)(|\kappa|^2-1)\end{aligned}$$

and thus we only need consider Schur iterates of $B_1(W)$ again. In this case $\gamma_2=X^2-V^2=(b-ac)(4a-b+ac)$ and $b-ac=2\mu(\cos\eta\,\Delta y-1)(p_0q_2-p_2)<0$ when $p_0q_2-p_2>0$. Hence the condition

$$\mu^2<\frac{p_0}{p_0q_2-p_2}$$

for $4a-b+ac=-(2/\mu)[2p_0+\mu^2(\cos\eta\,\Delta Y-1)(p_0q_2-p_2)]<0$. From (5.4)

$$\begin{aligned}\gamma_3&=(X^2-V^2)^2-(XZ-VY)^2\\&=(4a(bc-ac^2-d)((4a-b)(b-ac)+ad)\end{aligned}$$

and $bc-ac^2-d<0$, provided that $p_4+q_2(p_0q_2-p_2)<0$. Then $\gamma_3>0$ provided that $(4a-b)(b-ac)+ad>0$, which gives the condition

$$\mu^2<\frac{(p_2-p_0q_2)p_0}{p_0p_4+p_2(p_0q_2-p_2)}$$

for $p_0p_4+p_2(p_0q_2-p_2)<0$.

Now the sign of γ_4 depends on the sign of $(X+V+Z+Y)(X-V+Z-Y)$ which depends on $d(16a-4b+d)$. Since $d=-4p_4\mu^3(\cos\eta\,\Delta y-1)^2$ is negative when $p_4>0$, $16a-4b+d$ must also be negative. The polynomial in $x=\mu\sin(\eta\,\Delta y/2)$, $f(x)=p_0+p_2x^2+p_4x^4$ must then be positive, which it is whenever $p_2^2-4p_0p_4<0$ or $\mu^2<[-p_2-\sqrt{p_2^2-4p_0p_4}]/2p_4$ and $p_2^2-4p_0p_4>0$.

The case when $\eta\,\Delta y=0$ is exactly the same as in Theorem 5.4. ∎

In the above proofs we have not considered roots which have $|\kappa|=|z|=1$. Except in Theorems 5.2 and 5.3, we can solve for κ to get an expression $\kappa=-\Omega/\bar{\Omega}$, for $z=e^{i\theta}$, where $\Omega=\Omega(e^{i\theta})$. Therefore $|\kappa|=1$, $\arg\kappa=2\arg\Omega+\pi$ and, if $\Omega=x+i\tilde{y}\sin\theta$, $\arg\Omega=\tan^{-1}(\tilde{y}\sin\theta/x)$. This means that if $y=\tilde{y}\sin\theta$, and x are of the same sign, $\arg\kappa$ is negative, whereas if y and x are of different sign, $\arg\kappa$ is positive. Therefore if $\tilde{y}$ and x have the same sign, the sign of $\arg\kappa$ is different to the sign of $\arg z$, which means that generalised eigensolutions may exist.

Furthermore, the reflection coefficient for $|\kappa_1|=|\kappa_2|=|z|=1$ is given by $|B(\kappa_2, z)/B(\kappa_1, z)|$, where $\kappa_1=\bar{\kappa}_2$. Thus for

$$B=\kappa\bar{\Omega}+\Omega,\qquad R=\frac{e^{i\phi}\bar{\Omega}+\Omega}{e^{-i\phi}\bar{\Omega}+\Omega},$$

where $\kappa_1=e^{i\phi}$. Therefore,

$$\begin{aligned}|R|^2&=\frac{2|\Omega|^2+\Omega^2e^{-i\phi}+\bar{\Omega}^2e^{i\phi}}{2|\Omega|^2+\bar{\Omega}^2e^{-i\phi}+\Omega^2e^{i\phi}}\\&<1\end{aligned}$$

if and only if $8 \sin\theta\tilde{y}x < 0$. We conclude that generalised eigensolutions have $|R| < 1$ if they exist.

For method (2.15) the analysis is similar. We can show that $\kappa = \Omega/\bar{\Omega}$ and therefore $\arg\kappa = 2\arg\Omega$. Thus for $\Omega = \tilde{x}\cos\theta/2 + i\tilde{y}\sin\theta/2$, generalised eigensolutions may exist for $\tilde{x}\tilde{y} < 0$. Furthermore, since in this case $B = \kappa\bar{\Omega} - \Omega$, generalised eigensolutions which exist will again have $|R| < 1$.

To determine whether these generalised eigensolutions exist, we need to find Ω for each of the cases considered. For Eq. (2.12), $\Omega = -(a+1)e^{i\theta} + 2(a-\tilde{b}) + (1-a)e^{-i\theta}$ and $\tilde{y} = -2$, $x = -2a\cos\theta + 2(a-\tilde{b})$. Now $\tilde{y} < 0$ and x can take either sign. Thus unstable generalised eigensolutions with $|R| < 1$ may exist. For Eq. (2.15) we obtain $\Omega = 2\cos 3\theta/2 + 2(b-1)\cos\theta/2 + 2ia\sin 3\theta/2 - 2i(3a-c)\sin\theta/2$, and thus $\tilde{x} = 2[b - 4\sin^2\theta/2]$ and $\tilde{y} = 2(c - 4a\sin^2\theta/2)$, which again can take different signs. The method given by (2.17) may also have generalised eigensolutions with $|R| < 1$, since

$$\Omega = 2a\cos 2\theta + 2(b+d-4a)\cos\theta + 6a - 2b + 2i\sin\theta(4\sin^2\theta/2 - c).$$

Finally, for (4.10) $\Omega = 2a\cos 2\theta + 2(b-4a)\cos\theta + 6a - 2b + d + 2i\sin\theta(4\sin^2\theta/2 - c)$ and, again, generalised eigensolutions with $|R| < 1$ may exist. Observe that Renaut and Petersen [16] also demonstrated that method (2.10) may allow generalised eigensolutions for which $|R| < 1$. We observe that none of these statements are conclusive. We have merely shown that generalised eigensolutions may exist. Numerical tests were also performed in each case to test whether, in the cases where $(\arg\kappa)\times(\arg z) < 0$, Eq. (2.11) is also satisfied. The numerical search found modes satisfying both the boundary equation and the interior equation for all of (2.10), (2.12), (2.17), and (4.10). Thus we conclude that, in all of these cases, generalised eigensolutions exist. For (2.10), however, the only generalised eigensolutions that were found were for values of μ larger than the maximum allowable μ. For (2.12) and (4.10) we only found generalised eigensolutions for the Newman boundary conditions and $\mu = 0.1$ or $\mu = 0.3$. The number of eigensolutions increases as we reduce the accuracy requirements in the search, but in every case there are significantly more results for the (2.17) method. In this latter case more generalised eigensolutions were found for $\mu = 0.1$, 0.2, or 0.3.

This just leaves method (2.13) for which $\kappa = 1 + i(4a\sin^2\theta/2 + 2\tilde{b}/\sin\theta)$. Therefore $|\kappa| > 1$ and no generalised eigensolutions exist.

6. NUMERICAL COMPUTATIONS

Here we give the result of some numerical tests which were designed to test and compare the boundary conditions described in this paper. The first experiments were designed to test the stability limits predicted by the theorems of Section 5. Our computations were designed similarly to those described in Higdon [8, 10]. In all tests we used a mesh size $\Delta x = \Delta y = 0.04$ and $c = 1$. The value of $\mu = c\,\Delta t/\Delta x$ was varied to find the values of μ for which the boundary condition is stable. The initial condition was taken to be

$$u(x, y, 0) = e^{-200r^2}, \tag{6.1}$$

where $r^2 = y^2 + (x - 0.52)^2$. This is similar to the test used by Higdon, but we used a sharper Gaussian in order that the support of the initial condition is a smaller domain. Initially a less sharp Gaussian was used, but we found that the domain on which we calculated the soslution needed to be significantly larger in order to keep the support of the initial condition away from the boundary. This led to prohibitive costs of computing when we attempted to follow the solution to look for instability. Initial tests, however, using a less sharp Gaussian did not show any signsificant differences to the results which we will report here.

To test stability we computed solutions to the wave equation on the domain

$$\Omega_1 = \{(x, y): -80 < x < 0.52, -80 < y < 0\}.$$

At $x = 0.52$ and $y = 0$ we imposed symmetry so that these boundaries could be ignored. Tests were run so that waves did not reach the boundary with $y = -80$ and so that waves reflected from $x = -80$ could not influence the results. This also means that there are effectively no corners in the problem which, as demonstrated by Engquist and Majda [3], can influence the stability of the problem. It was our intent here to test the stability limits derived in Section 5, which do not include any analysis of corner interactions. The effects of corners on stability will be investigated in later work. We then compared these solutions with solutions found on the domain

$$\Omega_2 = \{(x, y): 0 < x < 0.52, -80 < y < 0\},$$

where we imposed various boundary conditions at $x = 0$. The computations thus test the reflection properties of the boundary conditions at $x = 0$, without interference from any other boundary. The regions Ω_1 and Ω_2 are large so that instabilities are given long enough to develop. It is our experience that instabilities may not show up on the usual smaller test regions. L_2-norms of the reflection on Ω_2 by subtracting the supposedly accurate solution on Ω_1, were calculated at regular time intervals. Instability was noted when these reflections grew unboundedly with time. Note here that what we are thus measuring is instability in the L_2 norm rather than GKS stability which is concerned with

stability as $\Delta t \to 0$. In fact the GKS stability permits exponential growth of solutions and, thus, an unbounded L_2-norm as $t \to +\infty$ does not necessarily imply GKS instability, although linear growth in the number of time steps as $\Delta t \to 0$ would imply GKS instability. The GKS stability requirement is, however, more stringent than L_2 stability and Trefethen [20] has also demonstrated that most GKS unstable difference schemes are also susceptible to unstable growth in the L_2-norm. Furthermore, in [5] it is conjectured that GKS stability implies L_2-stability. Results of these tests are summarized in Table III, where we give the range of Courant values for which each boundary condition studied in Section 5 may be stable. If a lower bound is not given, it is assumed to be zero. We also tested the Lindman condition and did not observe any instability for $\mu < 1/\sqrt{2}$, the bound on μ for stability of the interior scheme.

From Table III we see that the theorems of Section 5 accurately predict the maximum Courant number that can be used for a stable result. Since in all cases, where Table II predicts that the bound on μ due to the boundary is less restrictive than that due to the interior, stable results are achieved with $\mu = 0.7$, near the $1/\sqrt{2}$ bound. But, where Table II predicts a more restrictive bound on μ, this is reflected in the values in Table III. Method (2.17), however, exhibits instability for small Courant numbers. It is clearly unstable at $\mu = 0.1$ in all cases but the growth in error for $\mu = 0.2$ is slow. In Section 5 we showed that generalised eigensolutions might exist in all cases except (2.13). Their existence was confirmed except for (2.15) by numerical search.

Although the existence of generalised eigensolutions must explain the unstable behaviour observed in (2.17) at $\mu = 0.1$, clarification of the apparently stable or only marginally unstable behaviour in other cases is required. For example, (2.17) exhibits generalised eigensolutions for $\mu = 0.7$ as do (4.10) and (2.12) for $\mu = 0.1$ and $\mu = 0.3$. In these cases instability is not apparent, but the boundary conditions are not as effective as would be expected from the other results. This may be explained by considering the different types of GKS instability that can occur. In Trefethen [22] it is shown that for the first-order hyperbolic equation the violation of the GKS stability criterion can cause mild instabilities in which the solution grows linearly in, or as the square root of, the number of timesteps. The minimum growth rate is determined by whether the solution is forced by boundary data or just by the initial condition. Furthermore, infinite reflection coefficients compound the problem. Finite reflection coefficients and zero boundary data produce the mildest instability. In the tests we performed, not only was $|R| < 1$ but it satisfied $|R| \ll 1$. Also, there was no applied forcing at the boundary. We might, therefore, expect to see only mild instabilities in all cases. This is not observed; the amplification is much more severe in a few cases. This difference may occur, for example, because there are more generalised eigensolutions which cumulatively contain more energy and, thus, cause greater amplification.

The second set of computations was designed to compare the effectiveness of stable boundary conditions, ignoring the effects of corners. The initial condition was defined by (6.1) but with $r = (x-0.5)^2 + y^2$. Solutions were found on the domains

$$\Omega_1 = \{(x, y): -1 < x < 2, -2 < y < 2\}$$

TABLE III

Observed Stability Bounds

	Approximation						
Method	Padé	L_x^∞	Chebyshev points	L^2	C-P	Newman points	L^∞
2.10	0.7	0.7	0.65	0.67	0.58	0.5	0.5
2.12	0.7	0.7	0.7	0.7	0.7	0.7	0.7
2.13	0.7	0.7	0.7	0.7	0.7	0.7	0.7
2.15	0.7	0.7	0.7	0.7	0.7	0.7	0.7
2.17	0.3–0.7	0.3–0.7	0.3–0.7	0.3–0.7	0.3–0.7	0.3–0.7	0.3–0.7
4.10	0.7	0.7	0.7	0.7	0.7	0.7	0.7
Lindman	0.7	0.7	0.7	0.7	0.7	0.7	0.7

TABLE IVa

Maximum Reflection on Time Interval 0–1.96 as a Percentage of the Initial Energy

	Approximation						
Method	Padé	L_x^∞	Chebyshev points	L^2	C-P	Newman points	L^∞
2.13	15.37	15.49	17.50	17.23	18.02	22.90	18.59
2.10	7.63	7.56	6.96	6.99	7.04	7.62	7.53
2.12	4.80	4.60	2.52	2.56	3.06	10.14	4.53
2.15	2.74	2.10	1.49	1.51	1.72	2.46	2.34
2.17	1.28	3.30	6.83	10.51	10.59	14.49	16.29
4.10	1.71	1.18	1.24	1.38	1.42	1.66	1.81
Lindman	1.23						

TABLE IVb

Final Reflection at Time 1.96 as a Percentage of Initial Energy

	Approximation						
Method	Padé	L_x^∞	Chebyshev points	L^2	C-P	Newman points	L^∞
2.13	6.31	6.40	7.64	7.49	7.94	10.19	8.25
2.10	3.66	3.66	4.04	3.97	4.32	4.87	4.90
2.12	1.68	1.60	1.37	1.28	1.58	4.32	1.89
2.15	1.17	1.07	0.81	0.79	0.79	1.13	1.13
2.17	1.07	2.61	5.27	6.50	6.47	6.40	6.45
4.10	0.88	0.76	0.80	0.82	0.84	0.83	0.86
Lindman	0.79						

and $\Omega_2 = \{(x, y) : 0 < x < 2, -2 < y < 2\}$. A time interval $0 \leqslant t \leqslant 1.96$ was actually used in the numerical computations. In this time the wave reaches the boundaries at $x = -1$, $x = 2$, and $y = \pm 2$. Thus the measurements were actually on the smaller domain defined by $\{(x, y) : 0 \leqslant x \leqslant 1, -1.52 \leqslant y \leqslant 1.52\}$. In this way the reflection due to the $x = 0$ boundary was determined.

We carried out calculations using all of the boundary conditions described in Section 2 so that we could see how the order of the approximation affected the reflection. For the second-order approximations this also tested how the

of the operator. Then we also tested the Higdon operator which interpolated at either two or three angles chosen to fit with $k = 2$ or $k = 3$ approximations of Section 2. For each of these we also compared results for $a = b = \frac{1}{2}$ and $a = b = \frac{1}{4}$. Finally we compared reflections with the Lindman boundary condition which has the smallest theoretical reflection coefficient of all schemes considered here. In each case we found the maximum amount of reflection in the time interval $0 < t < 1.96$ and the amount of reflection at the end of the run. These values, for a Courant number of $\mu = 0.7$, are given in Tables IVa, IVb, Va, and Vb where the methods of Section 2 are given in Table IV and the Higdon schemes in Table V. Tests were made for Courant numbers between 0.1 and 0.7 in steps of 0.1. Here we present results for $\mu = 0.7$, because there was no appreciable difference in the comparison at different Courant numbers. The numbers given represent the percentage of energy reflected relative to the initial energy on Ω_2.

Table IVa compares the maximum reflection of the rational approximation methods. The first-order approximation (2.13) to the second-order paraxial approximation is clearly less effective than either of the second-order approximations. The new second-order stencil (2.12) is also better than (2.10) with the error reduced by about 50–60% in most cases. From Table IVb we can see that the final

(2.15) represents about a 40% improvement over (2.12) and (4.10) reduces the maximum error that occurs yet further. If we compare the final error, however, we see that in some cases (2.12) performs a little better than (4.10). Clearly the discretization (2.17) of the $k = 4$ methods is not effective. Finally, observe that the Lindman method performs just a little better than $k = 4$ except for the L_α^∞ approximation.

Tables Va and Vb compare the Higdon operators using either $a = b = \frac{1}{4}$ or $a = b = \frac{1}{2}$. The interpolating angles are chosen to be the same as the interpolating angles of the equivalent approximations. In almost all cases the choice $a = b = \frac{1}{2}$ gives least error. Comparing (2.12) and $p = 2$, $a = b = \frac{1}{2}$, we see that either implementation is satisfactory, the results are very close. With three points of interpolation (2.15) is a little better, in general, than the Higdon operator. Observe, however, that the final error is minimal for the $p = 3$ Higdon operator when compared with the L^2 and Chebyshev approximations.

TABLE Va

Maximum Reflection on Time Interval 0–1.96 as a Percentage of Initial Energy

	Approximation						
Method	Padé	L_α^∞	Chebyshev points	L^2	C-P	Newman points	L^∞
$p = 2$							
$a = b = \frac{1}{4}$	4.79	4.57	3.90	3.53	5.04	12.69	7.12
$a = b = \frac{1}{2}$	5.07	4.51	2.64	2.67	3.44	11.22	5.33
$p = 3$							
$a = b = \frac{1}{4}$	9.76	9.18	8.17	8.05	7.85	7.70	7.65
$a = b = \frac{1}{2}$	3.15	2.37	1.75	1.78	2.16	3.30	2.41

TABLE Vb

Final Reflected Energy at Time 1.96 as a Percentage of Initial Energy

	Approximation						
Method	Padé	L_α^∞	Chebyshev points	L^2	C-P	Newman points	L^∞
$p = 2$							
$a = b = \frac{1}{4}$	2.06	1.96	1.99	1.84	2.43	5.75	3.15
$a = b = \frac{1}{2}$	1.60	1.52	1.33	1.24	1.60	4.42	2.01
$p = 3$							
$a = b = \frac{1}{4}$	3.65	3.41	3.03	2.96	2.90	2.88	2.81
$a = b = \frac{1}{2}$	1.21	1.08	0.72	0.67	0.70	1.26	1.10

7. CONCLUSIONS

In this paper we have demonstrated how absorbing boundary conditions derived from approximations to the one-way wave equation may be discretised. A technique based on the Schur criteria can be applied to obtain necessary conditions for GKS stability. Numerical experiments reported in Section 6 confirm these upper bounds on μ. The existence of wavelike solutions which can cause instability is determined by numerical search. Their effects are seen in varying degrees in the numerical tests. From these tests we conclude that our approach for finding difference approximations, which is based on Lindman's ideas, leads to methods which exhibit few wavelike solutions compared to a difference approximation derived in a direct manner. In fact, wavelike solutions are only evident for small values of μ and the Newman boundary conditions. We conclude that Eq. (2.15), (2.10), and (2.13) can be used for all μ, and (4.10) and (2.12) for all μ excluding the Newman case.

From the comparison of the effectiveness of the methods, we conclude that the order of the approximation is impor-

tant for reducing the maximum error that occurs. It appears, however, that the final error is not significantly reduced by increasing k. The reduction of the maximum error is important in practice. There is really little to choose between Higdon's operators and the rational approximation approach for $k = 2$. The $k = 3$ results indicate that the rational approximation approach may be preferable when we increase the number of points of interpolation. Lindman's scheme is really no better than some of the $k = 4$ operators. In particular, Lindman's method performs a little worse than the (4.10) discretisation for the L_α^∞ approximation and a little better than the (4.10) discretisation for the approximation using Chebyshev points. It may, however, be possible to design schemes to the inverse square root that out perform the approximations to the square root. This is a problem that we will consider in the future. We note, also that Lindman's scheme is stable but not, we believe, because $|\beta_i| < 1$ as stated in [14]. We have looked at simpler Lindman schemes and derived stability conditions which do not require $|\beta_i| < 1$.

Note that our computations reported here were not intended for comparison between approximations. It has already been demonstrated by Renaut and Petersen [16] that the theoretical reflection coefficients accurately predict the numerical results when the difference operator is stable. Therefore the choice of approximation should be determined by the range of angles for which good absorption is required. For a given approximation, low or high order implementations are possible. Since the high order implementation, $k = 4$, requires only a little more computation than the $k = 2$ case and, because the increased order improves the effectiveness of the absorbing boundary significantly, the $k = 4$ should, in general, be chosen. It is assumed that implementations based on Lindman's approach be chosen because of their better stability properties.

ACKNOWLEDGMENTS

The author is grateful to R. Higdon and to two unknown referees for many helpful suggestions and comments.

REFERENCES

0. O. Buneman, Starlab, Stanford University, CA, private communication (1989).
1. C. Cerjan, D. Kosloff, R. Kosloff, and M. Reshef, *Geophysics* **50**, 705 (1985).
2. R. Clayton and B. Engquist, *Bull. Seismol. Soc. Am.* **67**, 1524 (1977).
3. B. Engquist and A. Majda, *Commun. Pure Appl. Math.* **32**, 313 (1979).
4. C. I. Goldstein, *Math. Comput.* **36**, 387 (1981).
5. B. Gustafsson, H. O. Kreiss, and A. Sundström, *Math. Comput.* **26**, 649 (1972).
6. L. Halpern and L. N. Trefethen, *J. Acoust. Soc. Am.* **84**, 1397 (1988).
7. P. Henrici, *Applied and Computational Complex Analysis, I* (Wiley, New York, 1974), p. 491.
8. R. L. Higdon, *Math. Comput.* **47**, 437 (1986).
9. R. L. Higdon, *SIAM Rev.* **28**, 177 (1986).
10. R. L. Higdon, *Math. Comput.* **49**, 65 (1987).
11. R. L. Higdon, *SIAM J. Numer. Anal.* **27**, 831 (1990).
12. J. B. Keller and D. Givoli, *J. Comput. Phys.* **82**, 172 (1988).
13. H. O. Kreiss, *Commun. Pure Appl. Math.* **23**, 277 (1970).
14. E. L. Lindman, *J. Comput. Phys.* **18**, 66 (1975).
15. C. J. Randall, *Geophysics* **53**, 611 (1988).
16. R. A. Renaut and J. Petersen, *Geophysics* **54**, 1153 (1989).
17. R. A. Renaut, *Frontiers Appl. Math. SIAM*, to appear.
18. A. C. Reynolds, *Geophysics* **43**, 1099 (1978).
19. W. D. Smith, *J. Comput. Phys.* **15**, 492 (1974).
20. L. N. Trefethen, Thesis, Stanford Computer Science Report No. STAN-CS-82-905, 1982 (unpublished).
21. L. N. Trefethen, *J. Comput. Phys.* **49**, 199 (1983).
22. L. N. Trefethen, *Commun. Pure Appl. Math.* **37**, 329 (1984).
23. L. N. Trefethen and L. Halpern, *Math. Comput.* **47**, 421 (1986).